Performance Degradation of the Block IV Telemetry System Due to the Presence of a CW Interference

M. K. Sue
Telecommunications Systems Section

The presence of an in-band CW interference can seriously degrade the performance of a telemetry system. Degradation effects for a phase-shift keying (PSK) system can be found in Refs. 1 and 2. The telemetry system employed for deep-space communications is a binary phase-shift keying system (BPSK) with squarewave subcarriers. The use of squarewave subcarriers makes the system less sensitive to in-band interference than a system using sinusoidal subcarriers. A model that allows one to predict the telemetry degradation for the deep-space telemetry system is presented in this article, backed with experimental data.

I. Introduction

This study is part of a continuing effort to investigate the adverse effects that a radio frequency interference (RFI) may have on the Deep Space Receiving System. Depending on the frequency and power level, an RFI can have various effects on the receiving system such as saturating receiver components, generating harmonics and degrading system performance. The saturation effects and the performance degradation of the carrier tracking loop have been documented (Refs. 3, 4) for the Block IV Receiving System. The purpose of this report is to examine the performance degradation of the Block IV telemetry channel due to in-band as well as out-of-band interference. An in-band interference, often called co-channel interference, is one whose frequency falls in the telemetry channel which is assumed to have a bandwidth on the order of twice the subcarrier frequency. An out-of-band interference is one that is not a co-channel one. This includes adjacent channel interference and interference that is remote from the desired channel frequency. An interference outside the telemetry channel can affect the telemetry channel performance; but the effects of an in-band interference are most severe.

An interference to the telemetry channel can produce two kinds of degradation effects. A strong interference can cause the telemetry Subcarrier Demodulation Assembly (SDA) and/or the Symbol Synchronization Assembly (SSA) to lose lock, resulting in a total loss of data. At a weaker level, an interference can increase the telemetry bit error rate. This report analyzes only the latter. The former will be examined in future articles.

II. Analysis

The effect of an in-band interference is first to be analyzed. Figure 1 shows a simplified functional block diagram of the Block IV telemetry receiving system. If we let $S(t)$ and $I(t)$ denote the received signal and interference respectively, then

$$S(t) = \sqrt{2}A \sin(\omega_c t + m\, p(t)\, d(t) + \theta) \quad (1)$$

and

$$I(t) = \sqrt{2}B \sin(\omega_c t + \omega_{sc} t + \Delta\omega t + \phi) \quad (2)$$

where A is the rms voltage of $S(t)$, B is the rms voltage of $I(t)$, ω_c is the carrier frequency in radians per second, $p(t)$ is the subcarrier, $d(t)$ is a binary data stream, $\Delta\omega$ is the RFI offset frequency in radians per second relative to the telemetry subcarrier frequency (ω_{sc}), θ is the phase angle of $S(t)$ m is modulation index and ϕ is the phase angle of $I(t)$, assumed to be a random variable uniformly distributed over $(0,2\pi)$. It is noted that $\Delta\omega$ is positive when the interference frequency is larger than $(\omega_c + \omega_{sc})$. The angular frequency of $I(t)$, ω_i is equal to the sum of ω_c, ω_{sc} and $\Delta\omega$.

The subcarrier $p(t)$ used for deep-space communications is a squarewave subcarrier and can be represented by Fourier series expansion,

$$p(t) = \sum_{k=1}^{\infty} \frac{4}{\pi(2k-1)} \sin((2k-1)\omega_{sc} t) \quad (3)$$

If we let $X_I(t)$ denote the input to the receiving system, then we have:

$$X_1(t) = \sqrt{2}A \sin(\omega_c t + mp(t)\, d(t) + \theta) + \sqrt{2}B \sin(\omega_i t + \phi) + n_1(t) \quad (4)$$

where $n_I(t)$ denotes the white Gaussian noise process with one-sided spectral density N_0.

The interference-to-signal ratio (ISR), which is an important parameter in determining the interference effects, is defined as follows:

$$ISR = P_I/P_D \quad (5)$$

where P_I denotes the power of the interference and P_D denotes the power of the telemetry. From Eqs. (1) and (2), we have:

$$P_I = B^2 \quad (6)$$

$$P_D = A^2 \sin^2(m) \quad (7)$$

Substituting Eqs. (6) and (7) into Eq. (5), we have:

$$ISR = \left(\frac{B}{A \sin(m)}\right)^2 \quad (8)$$

It is noted that ISR as defined in Eqs. (5) and (8) is referenced at the receiver input. Another parameter that is of importance is the energy per symbol to noise spectral density ratio, ST_s/N_0, defined as follows:

$$\frac{ST_s}{N_0} \triangleq \rho_s = \frac{P_D T_s}{N_0} = \frac{\left(A \sin(m)\right)^2 T_s}{N_0} \quad (9)$$

The first operation that the receiving system performs is carrier tracking, where the carrier phase is tracked by a phase locked loop and a locally generated reference signal $r_1(t)$ is created. Assuming perfect tracking, $r_1(t)$ can be written as follows:

$$r_1(t) = 2\cos[(\omega_c - \omega_{IF})t + \theta] \quad (10)$$

where ω_{IF} represents the IF frequency in radians per second.

This reference signal is used to downconvert $X_1(t)$ to IF frequency (see Fig. 1). Denoting the downconverted signal by $X_2(t)$ and ignoring double frequency terms and expressing the interference frequency in terms of ω_{IF}, ω_{sc} and $\Delta\omega$, we have

$$X_2(t) = \sqrt{2}A \cos(m) \sin(\omega_{IF} t) + \sqrt{2}A \sin(m) \cos(\omega_{IF} t)\, p(t)\, d(t) + \sqrt{2}B \sin\left((\omega_{IF} + \omega_{sc} + \Delta\omega)t + \phi - \theta\right) + n_2(t) \quad (11)$$

where $n_2(t)$ is the filtered noise process at IF frequency with one-sided spectral density N_0.

The subcarrier tracking loop then tracks the subcarrier and generates a subcarrier reference signal. Ignoring subcarrier

tracking error, then the subcarrier reference $r_2(t)$ is identical to $p(t)$; i.e.,

$$r_2(t) = p(t) = \sum_{k=1}^{\infty} \frac{4}{\pi(2k-1)} \sin((2k-1)\,\omega_{sc}t). \tag{12}$$

The subcarrier reference signal is then used to demodulate $X_2(t)$.

Denoting the demodulated signal by $X_3(t)$, i.e.,

$$X_3(t) = X_2(t)\, r_2(t) \tag{13}$$

and substituting Eqs. (11) and (12) into Eq. (13), we have

$$\begin{aligned} X_3(t) = {} & \sqrt{2}A \cos(m) \sin(\omega_{IF}t) \cdot \\ & \sum_{k=1}^{\infty} \frac{4}{\pi(2k-1)} \sin[(2k-1)\omega_{sc}t] \\ & + \sqrt{2}A \sin(m) \cos(\omega_{IF}t)\; d(t) \cdot \\ & \sum_{j=1}^{\infty} \sum_{k=1}^{\infty} \frac{16}{\pi^2(2k-1)(2j-1)} \begin{Bmatrix} \sin[(2k-1)\omega_{sc}t] \cdot \\ \sin[(2j-1)\omega_{sc}t] \end{Bmatrix} \\ & + \sqrt{2}B \sin((\omega_{IF} + \omega_{sc} + \Delta\omega)\, t + \phi - \theta) \cdot \\ & \sum_{k=1}^{\infty} \frac{4}{\pi(2k-1)} \sin[(2k-1)\omega_{sc}t] \\ & + n_3(t) \end{aligned} \tag{14}$$

The second term in Eq. (14) is the desired telemetry signal and can be reduced to $\sqrt{2}A \sin(m) \cos(\omega_{IF}t)\, d(t)$ because the result of the double summation is unity. The noise process is represented by $n_3(t)$. The output of the mixer $X_3(t)$ is then filtered by a predetection filter (PDF). This filter is assumed to be an ideal filter that passes all in-band signals and completely rejects out-of-band signals. Ignoring interference and carrier components more than $\omega_{sc}/2\pi$ hertz from the IF frequency, the predection filter output is:

$$\begin{aligned} X_4(t) = {} & \sqrt{2}A \sin(m)\, d(t) \cos(\omega_{IF}t) \\ & + \frac{2\sqrt{2}}{\pi} B \cos[(\omega_{IF} + \Delta\omega)\, t + \phi - \theta] \\ & + n_4(t) \end{aligned} \tag{15}$$

where $n_4(t)$ is the filtered noise process. If we ignore the broadening of the noise spectrum due to the multiplication of $n_2(t)$ by $r_2(t)$ in Eq. (13), then the one-sided noise spectral density of $n_4(t)$ is approximately equal to N_0.

We have assumed in Eq. (15) that the interference component at $\omega_{IF} + \Delta\omega$ is inside the passband of the filter so that there is no attenuation caused by filtering. This assumption requires that $\Delta\omega$ be small compared to the bandwidth of the predetection filter and it represents a worst case condition.

After subcarrier demodulation the signal is multiplied by a coherent 10 MHz reference signal to downconvert $X_4(t)$ to baseband. Denoting this reference signal by $r_3(t)$, we have:

$$r_3(t) = \sqrt{2} \cos(\omega_{IF}t) \tag{16}$$

Ignoring the double frequency terms, the output of the multiplier denoted by $X_5(t)$ is:

$$X_5(t) = A \sin(m)\, d(t) + \frac{2B}{\pi} \cos(|\Delta\omega|\, t + \phi - \theta) + n_5(t) \tag{17}$$

where $|\ |$ denotes the absolute value and $n_5(t)$ is the noise process at baseband with one-sided spectral density N_0.

The baseband signal including interference and noise components is then fed to the Symbol Synchronization Assembly (SSA) for symbol synchronization and symbol detection. Symbol detection is achieved using an integrate and dump circuitry.

Ignoring symbol synchronization error, the probability of symbol error P_s has been derived in Appendix A and is given in Eq. (18).

$$P_s = \frac{1}{2\pi} \int_0^{\pi} \operatorname{erfc}\left[\rho_c^{1/2} \left(1 + \frac{2}{\pi} R \cos\phi\right)\right] d\phi \tag{18}$$

where

$$\operatorname{erfc}(x) = \frac{2}{\pi} \int_x^{\infty} \exp(-y^2)\, dy.$$

and

$$R^2 = ISR.$$

Using a different approach, Rosenbaum (Ref. 2) has obtained an expression for the probability of symbol error for a PSK system under the influence of a CW in-band interference. The results of Ref. 2 differ from Eq. (18) by the multiplication factor $2/\pi$ in front of $R \cos \phi$. This factor is due to the use of squarewave subcarrier and it makes the telemetry system less sensitive to in-band CW interference by approximately 4 dB. Equation (18) indicates that the performance degradation in terms of increasing symbol error rate is independent of the symbol rate for a given ST_s/N_0 and a given R.

In the absence of interference, R equals zero and Eq. (18) becomes

$$P_s(R=0) = \frac{1}{2} \operatorname{erfc}(\rho_s^{1/2}) \tag{19}$$

which is the baseband error probability for coherent reception of PSK signals.

RFI degradation effects can be expressed in terms of an equivalent loss in ST_s/N_0. If we let $P_s(\rho_s, R)$ denote the probability of symbol error in the presence of an interference having an ISR equal to R^2 and a ST_s/N_0 equal to ρ_s, then the equivalent loss in ST_s/N_0 denoted by γ is

$$\gamma = \{\operatorname{erfc}^{-1}[2P_s(\rho_s, R)]\}^2/P_s \tag{20}$$

where erfc^{-1} denotes the inverse of erfc. Equations (18) and (20) represent our model for the prediction of uncoded telemetry performance degradation due to in-band CW RFI.

III. Experimental Verification

Equation (18) gives the symbol error performance as a function of ISR and ST_s/N_0 for a system with perfect carrier, subcarrier and symbol synchronization. A set of curves have been generated using Eqs. (18) and (20) and are shown in Figs. 2 and 3. Experimental verification of error rate curves was performed in TDL. A comparison of analytical and experimental data is shown in Fig. 4 after the observed ST_s/N_0 has been compensated for TDL system loss. The system loss, which is mainly caused by noise, includes losses due to errors in carrier tracking, subcarrier tracking and symbol synchronization. It was measured in the absence of interference by comparing the ST_s/N_0 required to obtain a given symbol error rate in TDL to the theoretical ST_s/N_0 corresponding to same error rate. The difference is taken as the system loss. As indicated in Fig. 4, TDL data agrees very well with theoretical data except at strong interference level (ISR = 0 dB) where the actual degradation is slightly more severe than predicted, by approximately 1 dB in interference to signal ratio. When the interference exceeds 0 dB, ISR total loss of data occurs due to loss of lock in SSA or SDA, or both.

The TDL measurements shown in Fig. 4 were based on a data rate of 115.2 kbps. Other data rates (10 and 50 kbps) had been tested and there was no noticeable difference in performance degradation. This is in agreement with the analysis (Eq. 18).

IV. Degradation on the Coded System

The effect of an in-band CW interference on the performance of a system using convolutional codes is difficult to analyze mathematically. Our derivation of the bit error expression under the influence of a CW interference is partly based on experimental observations. For the MCD (Maximum Likelihood Convolutional Decoding) implemented in the DSN, the probability of bit error in the absence of interference can be approximated by Eq. (21) (Ref. 5).

$$P_E(\text{No RFI}) \approx A \exp(B\rho) \tag{21}$$

where $A = 85.7501$, $B = -5.7230$ and ρ is the signal energy per bit to noise spectral density ratio (E_b/N_0). Equation (21) is applicable for $K = 7$, rate 1/2 convolutional codes with 3-bit quantization and $\rho = 2\rho_s$.

If we can estimate the effective signal energy per bit to noise spectral density ratio ρ_e, then Eq. (21) can be applied to estimate the probability of error under the influence of an interference. From Eq. (20), the effective signal to noise ratio for a given R and ρ_s can be modelled as

$$\rho_e = 2\{\operatorname{erfc}^{-1}[2P_s(\rho_s, R)]\}^2. \tag{22}$$

Substituting Eq. (22) for ρ in Eq. (21), the probability of bit error under the influence of a CW RFI is

$$P_E \approx A \exp(2B\{\operatorname{erfc}^{-1}[2P_s(\rho_s, R)]\}^2) \tag{23}$$

for a given R and ρ_s.

Since Eq. (23) is based on the analytical model for the uncoded case, i.e., Eqs. (18) and (20), the accuracy of Eq. (33) depends on the accuracy of Eq. (18) or (20). As previously mentioned, the analytical model for the uncoded case works

very well for ISR less than 0 dB. At 0 dB, the analytical model is about 1 dB less sensitive to RFI than the actual system. To account for this deficiency, it is necessary to modify Eq. (23) slightly by placing restrictions on its applicability.

$$P_E = \begin{cases} A \exp\left(2B\{\text{erfc}^{-1}\ [2P_s(\rho_s, R)]\}^2\right) & ISR < 0 \text{ dB} \\ A \exp\left(2B\{\text{erfc}^{-1}\ [2P_s(\rho_s, R^*)]\}^2\right) & ISR = 0 \text{ dB} \end{cases} \tag{24}$$

where 20 log R^* = 1 dB. Equation (24) represents our model for the prediction of telemetry performance degradation for the coded case due to in-band CW RFI.

A set of curves have been generated using Eq. (24) and they are shown in Fig. 5. Experimental verification was performed in TDL. To avoid the need for excessive testing time, the range of E_b/N_0 was limited to from 2 to 5 dB, excluding TDL system losses. This range of E_b/N_0 corresponds to a bit error rate of 10^{-2} to 10^{-6}, which approximately covers the normal DSN operating range. A comparison of TDL data to those predicted by Eq. (24) is shown in Fig. 6 and they are in good agreement.

V. Translation Effects

In the preceding analysis, we have assumed that the interference is an in-band interference; i.e., the frequency separation between the interference and the subcarrier frequency is on the order of the subcarrier frequency or less. Although the telemetry system is most sensitive to in-band interference, out-of-band interference can degrade telemetry performance through a process often termed as translation where an out-of-band interference gets multiplied by a subcarrier reference during the subcarrier demodulation process and creates an in-band interfering component that falls inside the passband of the predetection filter. If we let $I_i(t)$ denote the interference at the ith position of the receiver (see Fig. 1), then after subcarrier demodulation the interference becomes (Eq. 14):

$$I_3(t) = \sqrt{2B}|H(\omega_i)| \sin\left[(\omega_{IF} + \omega_{sc} + \Delta\omega)\, t + \phi - \theta + \phi_H(\Delta\omega)\right] \cdot \sum_{k=1}^{\infty} \frac{4}{\pi(2k-1)} \sin\left[(2k-1)\omega_{sc} t\right] \tag{25}$$

where $|H(\omega_i)|$ and $\phi_H(\omega_i)$ are the amplitude and phase of $H(j\omega)$ evaluated at ω_i and $H(j\omega)$ represents the transfer function of the first part of the receiver; i.e.,

$$H(j\omega) = \frac{x_2(j\omega)}{x_1(j\omega)}$$

where $x_1(j\omega)$ and $x_2(j\omega)$ are the Fourier transform of $x_1(t)$ and $x_2(t)$ respectively. In Eq. (14), $|H(\omega_i)|$ has been assumed to be 1.

For a given ω_i, the phase angle $\phi_H(\omega_i)$ is a constant and does not affect the outcome and thus can be ignored. The factor $|H(\omega_i)|$ in Eq. (25) represents the attenuation on the out-of-band interference. A plot of $|H(\omega)|$ as a function of frequency is shown in Fig. 7 for the Block IV receiver. The frequency response was measured in TDL.

It is obvious from Eq. (25) that a single CW RFI has been, through the process of subcarrier demodulation, decomposed into a set of interfering components each having a radian frequency ω_k and power P_k; $k = 1, 2, 3 \ldots$, where

$$\omega_k = \begin{cases} \omega_{IF} + \Delta\omega + 2k\omega_{sc} \\ \omega_{IF} + \Delta\omega - 2(k-1)\omega_{sc} \end{cases} \qquad k = 1, 2, 3 \ldots \tag{26}$$

and

$$P_k = \left[\frac{2B|H(\omega_i)|}{\pi(2k-1)}\right]^2 \qquad k = 1, 2, 3 \ldots \tag{27}$$

These interfering components are equally spaced at $2\omega_{sc}$ radians/sec apart. If we assume that the bandwidth of the predetection filter is on the order of $2\omega_{sc}$, then one of these components would fall inside the predetection bandwidth and would be passed practically without attenuation. The power of this interfering component at the predetection filter output is given by Eq. (27), with k being related to the interference frequency ω_i as follows

$$CPOI\left(\frac{\omega_i - \omega_C}{\omega_{sc}}\right) = 2k - 1 \tag{28}$$

where $CPOI(x)$ denotes the positive odd integer that is closest to x. If x is equidistant from two odd integers, the larger integer is arbitrarily assigned to $CPOI(x)$.

In order for out-of-band CW interference to produce the same degradation effect on the telemetry system as an in-band interference, it is obvious from Eqs. (27) and (28) that an

additional amount of interference power is needed to compensate for the attenuation due to the frequency response of the telemetry channel and the spreading effects due to multiplication by the subcarrier reference. If we let ΔP_K denote the additional power and P_1 denote the power level of an in-band interference at the predetection filter output, then

$$\Delta P_k \text{ (dB)} = 10 \log \frac{P_1}{P_k} \tag{29}$$

The power of an in-band interference at the filter output can be obtained from Eq. (15) or from Eq. (27) by setting $k = 1$ and $|H(j\omega)| = 1$,

$$P_1 = (2B/\pi)^2 \tag{30}$$

Substituting Eq. (30) and Eq. (27) into (29), we have

$$\Delta P_k \text{(dB)} = 20 \log [(2k - 1)/|H(\omega_i)|] \tag{31}$$

Eq. (31) when used in conjunction with Eqs. (18), (20) and (24) provides the necessary models to account for the effects of out-of-band interference.

Eq. (3) has been evaluated for selected frequencies as shown in Table 1. Experimental verification of the translation mechanism was performed in TDL using the Block IV receiver. The power level of an in-band interference required to produce a symbol error rate of 2.5×10^{-3} was first determined and used as a reference. (The symbol error rate was approximately 1.0×10^{-3} in the absence of interference.) The power level of an out-of-band interference was then adjusted to produce the same symbol error rate (2.5×10^{-3}). The additional power level was obtained by subtracting the reference power level from the power level of the out-of-band interference. TDL data are also included in Table 1; they are in good agreement with analytical data.

Table 1 reveals a potential RFI problem associated with the unique feature of the receiving system. The wide bandwidth of the telemetry channel offers good performance in a noisy environment, but leaves the telemetry channel open for out-of-band interference. As indicated in Table 1, a CW RFI with a moderate power level and at a frequency relatively remote from the frequency of the desired signal can produce significant performance degradation through the translation mechanism. At 2.5 MHz away, which corresponds to a frequency separation of about seven S-band channels in the DSN channel plan, a CW RFI needs to be only about 17 dB stronger than a co-channel interference in order to produce the same degradation. The protection against out-of-band interference is therefore considered to be inadequate with the existing system. Improvement in RFI immunity should be considered in future designs. Significant improvement would ease the problem of channel selection for future missions and allow more efficient use of band allocations.

VI. Conclusion

Telemetry performance degradation of the Block IV receiving system due to CW interference has been examined. The use of a square wave subcarrier instead of a sine wave has both advantage and disadvantage in terms of RFI protection. On one hand, it makes the system less sensitive to in-band CW interference by about 4.0 dB. On the other hand, it makes the system susceptible to out-of-band interference due to the translation mechanism. Despite simplifying assumptions in the analytical model, experimental data obtained in TDL indicate that the model is sufficiently accurate throughout nominal operating range. The telemetry degradation models are provided by Eqs. (18), (20) and (24) for in-band and out-of-band interference and for the coded and uncoded systems.

Acknowledgment

The author wishes to express his appreciation to J. F. Weese, who performed the experimental measurements in TDL, and D. R. Hersey for technical consultations.

References

1. Koerner, M. A., *Effect of Interference on a Binary Communication Channel Using Known Signals*, Technical Report 32-1281, Jet Propulsion Laboratory, Pasadena, Calif., Dec. 1, 1968.

2. Rosenbaum, A. S., "PSK Error Performance with Gaussian Noise and Interference," *Bell System Technical Journal*, Feb. 1969.

3. Hersey, D. R., and Sue, M. K., "Maximum CW RFI Power Levels for Linear Operation of the DSN Block IV Receiver at S-Band Frequencies," *DSN Progress Report 42-56, January and February 1980*, Jet Propulsion Laboratory, Pasadena, Calif. April 15, 1980.

4. Sue, M. K., "Block IV Receiver Tracking Loop Performance in the Presence of a CW RFI," *DSN Progress Report 42-60, September and October 1980*, Jet Propulsion Laboratory, Pasadena, Calif., Dec. 15, 1980.

5. Webster, L., "Maximum Likelihood Convolutional Decoding (MCD) Performance Due to System Losses," *DSN Progress Report 42-34*, Jet Propulsion Laboratory, Pasadena, Calif., Aug. 15, 1976.

Table 1. Additional interference power level required for an out-of-band CW interference to produce the same effect as an in-band interference (experimental results are based on a symbol error rate of 2.5×10^{-3} in the presence of an interference or 1.0×10^{-3} in the absence of it)

Interference frequency relative to carrier frequency $(\omega_i - \omega_c)/2\pi$ kHz	Value of k[1]	$\lvert H(\omega_i)\rvert^2$, dB	20 log(2k−1), dB	ΔP_K, dB	
				Predicted	Measured[2]
360	1	0	0	0	0
1080	2	0	9.5	9.5	10.1
1800	3	0	14.0	14.0	14.2
2520	4	0	17.0	17.0	17.2
3240	5	0	19.1	19.1	20.2
3960	6	−2.0	20.8	22.8	23.7
4690	7	−3.0	22.3	25.3	25.4
5400	8	−6.0	23.5	29.5	30.9
6120	9	−20.0	24.6	44.6	46.2
6840	10	−42.0	25.6	67.6	70.2

[1]Equation (28).
[2]Block IV receiver.

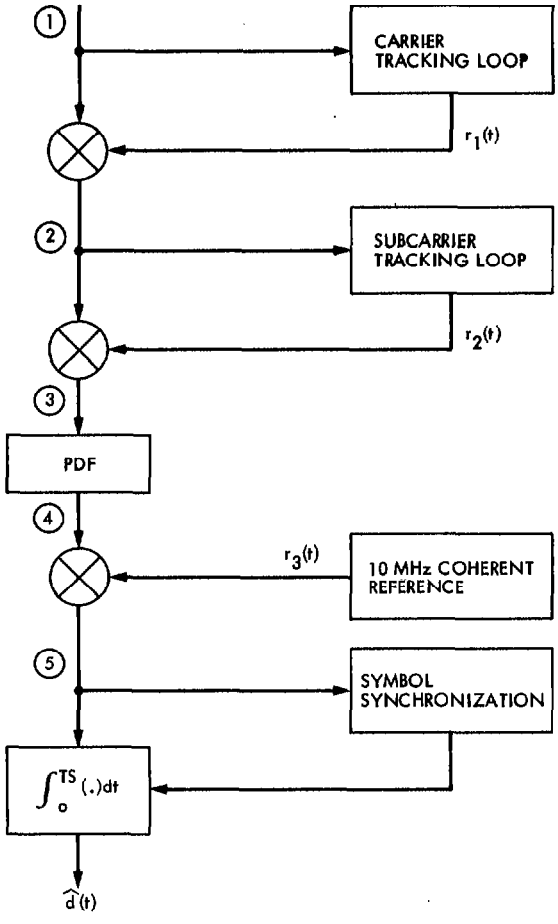

Fig. 1. Functional block diagram of the Block IV Telemetry Receiving System

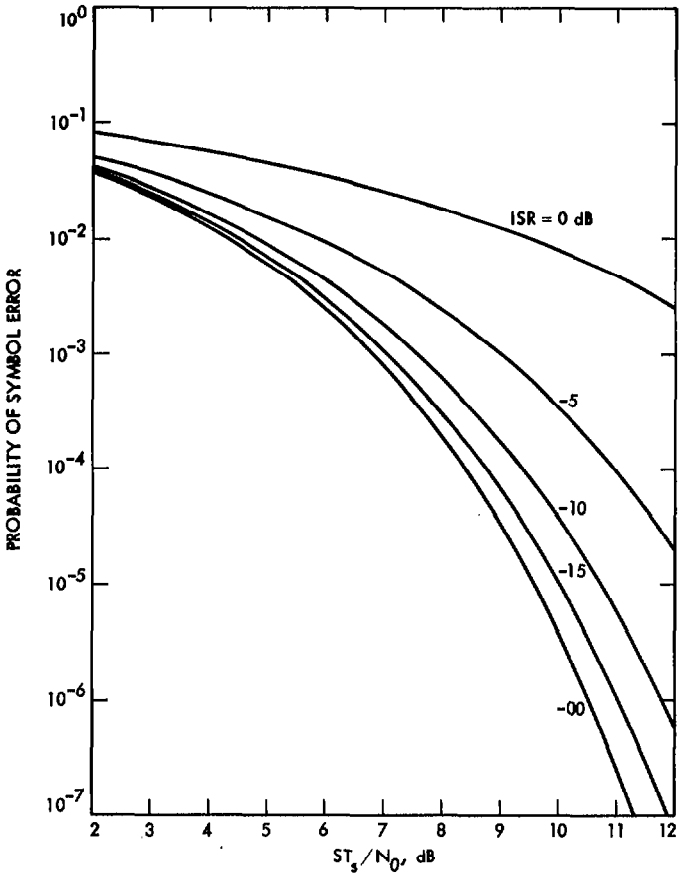

Fig. 2. Probability of symbol error vs ST_s/N_0

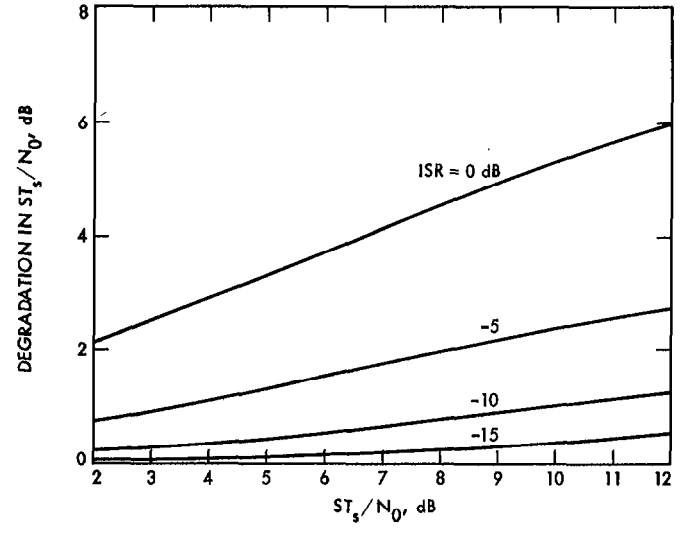

Fig. 3. Degradation in ST_s/N_0 vs ST_s/N_0, dB

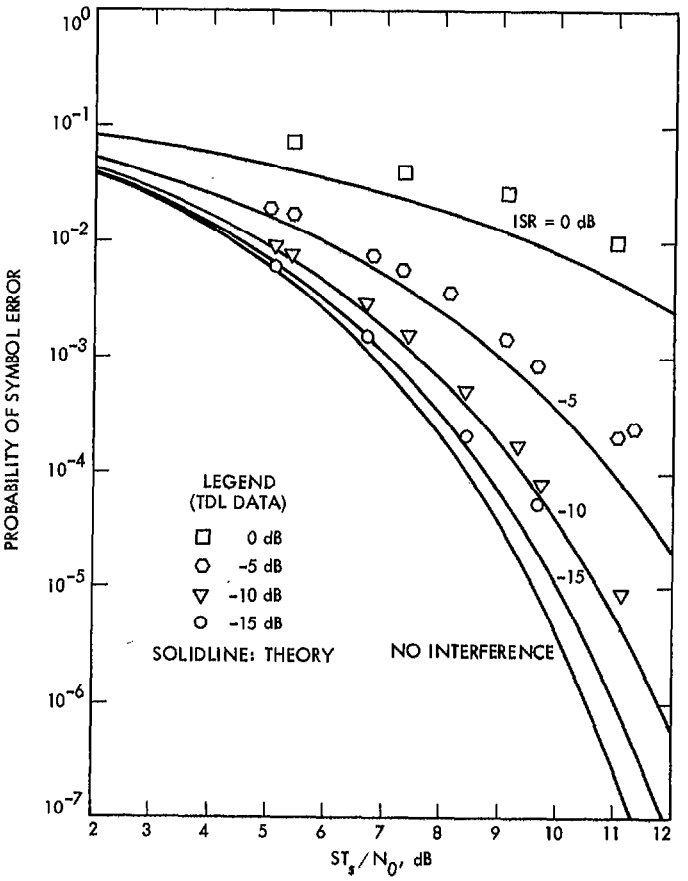

Fig. 4. Comparison of experimental and analytical results

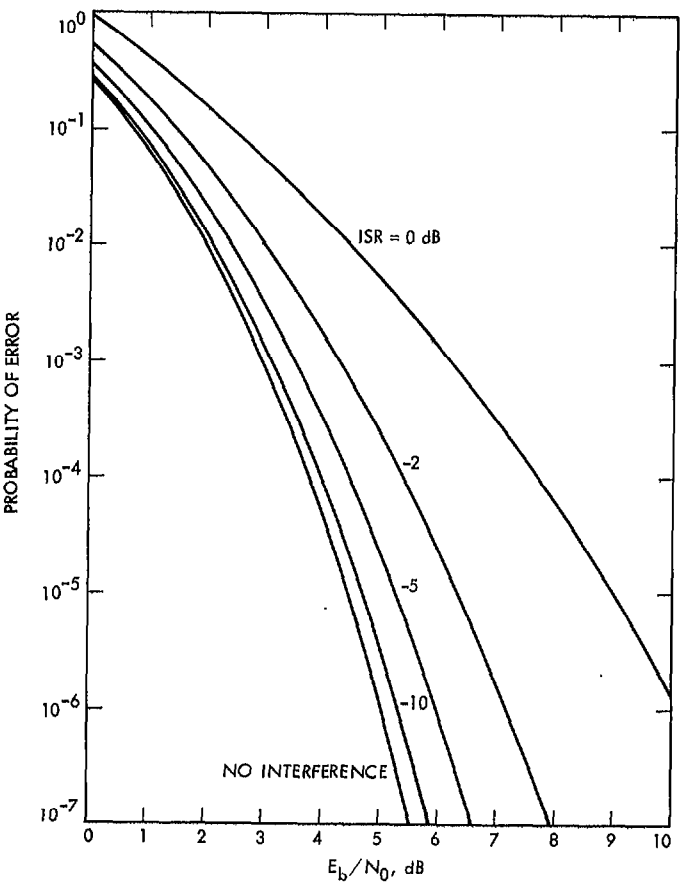

Fig. 5. Probability of bit error vs E_b/N_0 for selected values of ISR (Eq. 24)

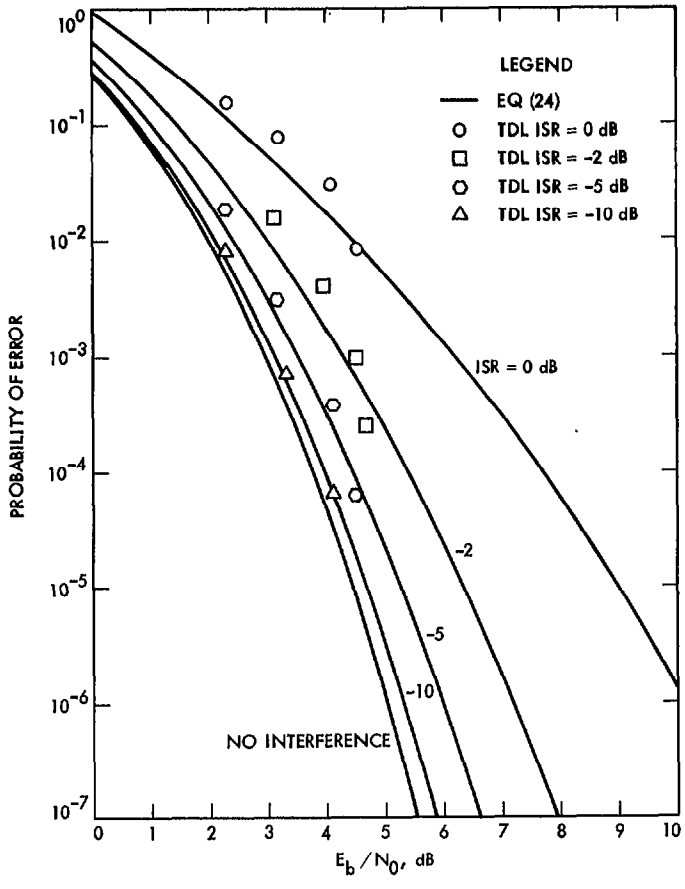

Fig. 6. Comparison of TDL and Eq. (24) results

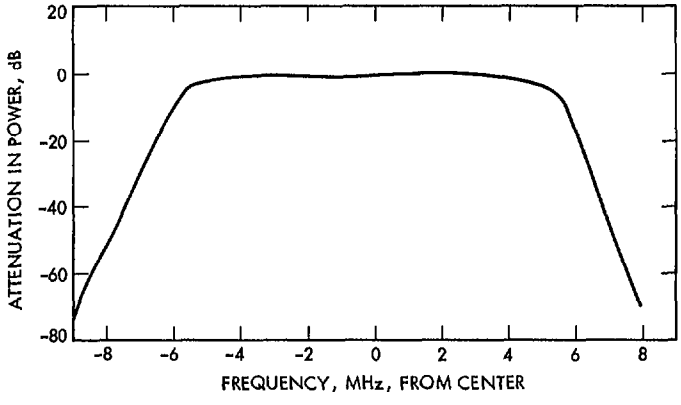

Fig. 7. TDL TLM channel frequency response vs frequency, Block IV receiver S-band (from receiver input to SDA input)

Appendix A

Derivation of Probability of Symbol Error

The probability of symbol error under the influence of a CW interference is derived in this appendix. The input to the data detector consists of three components: signal, interference and noise. Denoting the input by $y(t)$, we have from Eq. (17) the following expression:

$$y(t) = a\,d(t) + b\cos(|\Delta\omega|\,t + \phi - \theta) + n_5(t) \qquad \text{(A-1)}$$

where we have replaced $A \sin(m)$ in Eq. (17) by a in Eq. (A-1) and $2B/\pi$ by b. The noise process $n_5(t)$ is the same noise process as in Eq. (17) and is assumed to be Gaussian with a correlation function $R(\tau) = N_0/2\,\delta(\tau)$.

The data detector performs data detection by integrating $y(t)$ over one symbol period T_s and announces its decision $\hat{d}$ according to the following rule:

$$\hat{d} = \begin{cases} d_1 = 1 & \text{if } q \geqslant 0 \\ d_2 = -1 & \text{if } q < 0 \end{cases} \qquad \text{(A-2)}$$

where

$$q = \int_0^{T_s} y(t)\,dt \qquad \text{(A-3)}$$

The interference in Eq. (A-1) can be modeled as $b\cos\psi$ with ψ being a random variable uniformly distributed over $(0, 2\pi)$. To determine the probability of symbol error P_s, it is necessary to first determine the conditional statistics of q. It can be shown that for a given $\psi = \psi_0$ and $d(t) = d_1 = 1$, we have the following conditional statistics:

$$E[q|\psi_0, d_1] = (a + b\cos\psi_0)\,T_s,$$

$$VAR[q|\psi_0, d_1] = \frac{N_0}{2}T_s$$

and

$$p(q|\psi_0, d_1) = \frac{1}{\sqrt{\pi N_0 T_s}}\exp\left(-(q - (a + b\cos\psi_0)\,T_s)^2/N_0T_s\right) \qquad \text{(A-4)}$$

where $E[\ ]$, $VAR[\ ]$, $p[\ ]$ and T_s denote the expectation, variance, probability density function and symbol duration respectively.

The probability of making an error given that d_1 was transmitted is equal to the probability that q is less than 0; i.e.,

$$P_s(s|\psi_0, d_1) = \text{prob}(q < 0|\psi_0, d_1) = \int_{-\infty}^{0} p(q|\psi_0, d_1)\,dq \qquad \text{(A-5)}$$

where $P_s[\ ]$ denotes the symbol error probability conditioned on ψ_0 and d_1. After simplification Eq. (A-5) becomes:

$$P_s(s|\psi_0, d_1) = \frac{1}{2}\,\text{erfc}\left(\frac{(a + b\cos\psi_0)\,T_s}{\sqrt{N_0T_s}}\right) \qquad \text{(A-6)}$$

where

$$\text{erfc}(x) \triangleq \frac{2}{\sqrt{\pi}}\int_x^{\infty} exp(-y^2)\,dy$$

Similarly, the probability of making an error given that $d_2 = -1$ was sent is equal to the probability that q is greater than or equal to 0 and is equal to:

$$P_s(s|\psi_0, d_2) = \text{prob}(q \geqslant 0|\psi_0, d_2)$$

$$= \frac{1}{2}\,\text{erfc}\left(\frac{(a - b\cos\psi_0)\,T_s}{\sqrt{N_0T_s}}\right) \qquad \text{(A-7)}$$

If we assume equal probability of occurrence for d_1 and d_2, then the probability of symbol error averaged over $d(t)$ and conditioned on $\psi = \psi_0$ can be calculated as follows:

$$P_s(s|\psi_0) = \text{prob}(d(t) = d_1)\,P_s(s|\psi_0, d_1) + \text{prob}(d(t) = d_2)\,P_s(s|\psi_0, d_2)$$

$$= \frac{1}{4}\,\text{erfc}\left(\frac{(a + b\cos\psi_0)\,T_s}{\sqrt{N_0T_s}}\right) + \frac{1}{4}\,\text{erfc}\left(\frac{(a - b\cos\psi_0)\,T_s}{\sqrt{N_0T_s}}\right) \qquad \text{(A-8)}$$

The probability of symbol error can be obtained from $P_s(s|\psi_0)$ by averaging over ψ_0.

$$P_s(s) = \int_{\psi_0} P_s(s|\psi_0)\, p_\psi(\psi_0)\, d\psi_0.$$

$$= \frac{1}{8\pi}\int_0^{2\pi} \text{erfc}\left(\frac{(a + b\cos\psi_0)\,T_s}{\sqrt{N_0 T_s}}\right) d\psi_0$$

$$+\frac{1}{8\pi}\int_0^{2\pi} \text{erfc}\left(\frac{(a - b\cos\psi_0)\,T_s}{\sqrt{N_0 T_s}}\right) d\psi_0 \quad \text{(A-9)}$$

where $P_\psi(\ )$ is the probability density function of ψ.

The two terms on the right-hand side of the above equation are equal and can be combined to yield:

$$P_s(s) = \frac{1}{2\pi}\int_0^{2\pi} \text{erfc}\left(\frac{(a + b\cos\psi_0)\,T_s}{\sqrt{N_0 T_s}}\right) d\psi_0 \quad \text{(A-10)}$$

Expressing $P_s(s)$ in terms of A and B and substituting Eqs. (5) – (8) into the above equation, we have after simplification of the following:

$$P_s(s) = \frac{1}{2\pi}\int_0^{\pi} \text{erfc}\left(\rho_s^{1/2}\left(1 + \frac{2}{\pi} R\cos\psi_0\right)\right) d\psi_0 \quad \text{(A-11)}$$

where $R^2 = ISR$.